

$^{63,65}\text{Cu}$ indirect spin-spin coupling in $\text{La}_{1.85}\text{Sr}_{0.15}\text{CuO}_4$

R. E. Walstedt and S-W. Cheong

AT&T Bell Laboratories, 600 Mountain Avenue, Murray Hill, New Jersey 07974

(Received 1 December 1995)

Measurements of the nuclear spin-echo decay time constant T_{2G} for both ^{63}Cu and ^{65}Cu in $\text{La}_{1.85}\text{Sr}_{0.15}\text{CuO}_4$ are presented for sample temperatures ranging from 100 to 300 K. Using methods developed recently, these measurements are corrected for the effects of T_1 modulation and of spin-spin flip-flop transitions. The results are then compared with predictions based on Kramers-Kronig integration of recent neutron data, and extrapolations thereof, for $\chi''(\vec{q}, \omega)$. Using the foregoing results and calculated corrections for $\text{YBa}_2\text{Cu}_3\text{O}_7$, we also discuss the evaluation of these systems in terms of quantum disordered ($z=1$) vs overdamped ($z=2$) behavior in the phase diagram proposed by Sokol and Pines.

The combination of recent NMR and neutron-scattering data on $\text{La}_{2-x}\text{Sr}_x\text{CuO}_4$ (LSCO) with $x \approx 0.15$ makes this system a rich laboratory for the study of spin fluctuation effects in the highly correlated cuprate conductors. Neutron data for $\chi''(\vec{q}, \omega)$ are now available showing incommensurate peaks near $\vec{q} = (\pi, \pi)$ at energies from 1 up to 35 meV and temperatures ranging from helium up to 300 K.¹⁻³ Data for nuclear spin-lattice relaxation times T_1 have been reported for both ^{63}Cu (Refs. 4,5) and ^{17}O (Refs. 5,6) in this system. Further, a detailed analysis of indirect spin-spin coupling derived from spin-echo decay (T_{2G}) data at $T=100$ K has also been reported.⁷ These results allow, first, a direct and successful test of the fluctuation-dissipation relation between T_1 and $\chi''(\vec{q}, \omega)$ for the copper,⁵ and second, a test of the relative magnitudes of indirect nuclear spin-spin coupling among copper spins (Cu-Cu) and between copper and oxygen spins (Cu-O). Using the Pennington-Slichter⁸ formulation, the indirect couplings are calculated from estimates of $\chi'(\vec{q})$. These are derived, in turn, from the neutron data for $\chi''(\vec{q}, \omega)$ using the Kramers-Kronig (KK) relation. The echo decay results have by and large confirmed our expectations for the case of copper. However, the neutron data have also yielded startling surprises for both the copper and the planar oxygen.

Let us summarize the current situation briefly. For copper, one finds at $T \sim T_c$ essentially quantitative agreement between measured T_1 values and estimates based on absolute data for $\chi''(\vec{q}, \omega)$ derived from neutron scattering.^{1,5} However, recent neutron data³ show a steep decline in the incommensurate peak amplitude with temperature, so that by 300 K the contribution to $\chi''(\vec{q}, \omega)$ so determined yields a T_1 rate which is less than the measured values by a factor ~ 3 . This surprising result calls into question the relevance of these neutron data to the $^{63,65}\text{Cu}$ NMR results at higher temperatures. For ^{17}O , the traditional one-band model of transferred hyperfine couplings at the planar oxygen sites^{9,10} has been found to predict a $T_1(T)$ profile which is not observed.⁵

A similar dichotomy of behaviors has recently been reported for the indirect coupling (T_{2G}) effect in LSCO⁷ as well. The $^{63,65}\text{Cu}$ spin-echo decay rates are clearly dominated by the indirect coupling. At $T=100$ K these rates are found to correspond to values of $\chi'(\vec{q})$ extracted from the

neutron data for $\chi''(\vec{q}, \omega)$ using the KK relation. Adopting a high-frequency cutoff for $\chi''(\vec{q}, \omega)$ which is consistent with $^{63,65}\text{Cu}$ data for T_{2G} , one finds that a large Cu-O indirect spin-spin coupling is also predicted for this system. Unexpectedly, however, the ^{17}O spin echo decay can be accounted for quantitatively with dipolar coupling alone.⁷ Both this result and the foregoing one regarding the ^{17}O T_1 lead to the conclusion that the Cu-O transferred hyperfine coupling is much smaller than the total coupling reflected by the measured ^{17}O NMR shift. It follows that the ^{17}O shift and T_1 process must be dominated by some unknown and unforeseen agency.^{5,7}

In this paper we report measurements of T_{2G} for $^{63,65}\text{Cu}$ in LSCO at temperatures ranging from 100 up to 300 K. These data are corrected for dynamical effects as in Ref. 7, thus extracting values for the *static* decay constant T_{2GS} (Ref. 11) which we relate to the indirect coupling second moment by $\langle \Delta \omega^2 \rangle_{\text{ind}} = 2/T_{2GS}^2$. The results are compared with estimates of $\chi'(\vec{q})$ derived from neutron data as well as with similar NMR results for $\text{YBa}_2\text{Cu}_3\text{O}_7$ (YBCO) from the literature.¹² The T_{2G} results are also used to discuss the placement of LSCO in the magnetic phase diagram for cuprates proposed by Sokol and Pines (SP).¹³ In this connection, we also present calculated corrections⁷ to the echo decay data for YBCO,¹² finding that experimental results corrected to yield T_{2GS} suggest a different placement of YBCO in the phase diagram from that given by SP.

Measurements of T_{2G} were derived from spin-echo decay curves for $^{63,65}\text{Cu}$ taken using the same partially oriented sample of LSCO used in Refs. 5 and 7. Data were taken at the center of oriented powder NMR lines with the applied field along the c axis. Typical decay data with fitted curves are shown in Fig. 1 for ^{63}Cu . In order to extract the indirect coupling second moment from the raw data, three corrections are applied: (1) By far the largest is the direct spin-lattice relaxation of the echo which operates in parallel with the spin-spin decay as a factor $\exp(-2\tau/T_{1E})$. T_{1E} is estimated from ordinary T_1 data as well as from measurements of the anisotropy of T_1 .^{7,14} (2) A correction is put in for background echo intensity caused by unoriented sample material which relaxes more slowly than the oriented sample peak studied. This correction is small, but important, and is described in detail below. (3) Last, there is a correction of up to

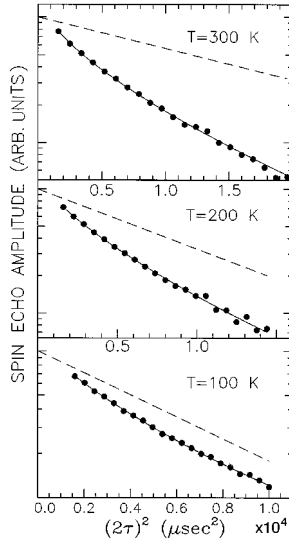


FIG. 1. Nuclear spin-echo decay data for ⁶³Cu in LSCO at three temperatures (dots), plotted vs $(2\tau)^2$, where τ is the spin-echo pulse separation. The solid lines are fitted curves based on Eq. (1) and the dashed lines are the spin-spin decay processes (assumed Gaussian) obtained in the fitting procedure for comparison.

25% from time modulation of the spin-spin couplings, both by flip-flop transitions caused by exchange-like terms in the indirect coupling,⁷ as well as by T_1 processes. The details of calculations to estimate these corrections are described in Ref. 7. We give some further results below.

We fit the raw echo decay data (Fig. 1) with the functional form

$$\mathcal{E}(2\tau) = A e^{-2\tau/T_{1Ec}} e^{-(2\tau)^2/T_{2G}^2} + B e^{-2\tau/T_{1E70}}. \quad (1)$$

The first term represents the oriented portion of the sample which has the field \vec{H} along the c axis. This term incorporates the (uncorrected) Gaussian decay rate τ_{2G}^{-1} due to indirect couplings which is to be measured. The exponential factor involving T_{1Ec} represents the direct spin-lattice relaxation process for the spin-echo amplitude. This time constant is calculated from $T_{1Ec}^{-1} = 3T_{1c}^{-1} + \frac{1}{2}(T_{1a}^{-1} + T_{1b}^{-1})$, where $T_{1\alpha}$ is the usually defined spin-lattice relaxation rate with the field in the α direction.^{7,12} Parameters for this factor are estimated from nuclear quadrupole resonance (NQR) T_1 data^{4,5} and the experimental result that $T_{1c}/T_{1ab} \approx 2.6$.⁴ We assume $T_{1a} \approx T_{1b}$.

The second term in Eq. (1) represents a background signal from unoriented sample material. For the relevant quadrupolar powder pattern, the c axis of crystallites for which the NMR frequency coincides with that of the oriented sample peak lies at an angle $\approx 70^\circ$ to the applied field. We estimate the Gaussian decay time for this orientation to be much longer and the direct T_1 process (T_{1E70}) to be much shorter, respectively, for the latter material than for the oriented portion. Accordingly, we include only the T_1 process for the background term, estimating T_{1E70} from data in the literature as described above. Line scans show that the background term represents about 10% of the measured amplitude at $T=300$ K, growing somewhat larger at low temperature. Fitting the data at $T=100$ K with the form in Eq. (1) gives a background amplitude of $\approx 20\%$. The parameter B is inter-

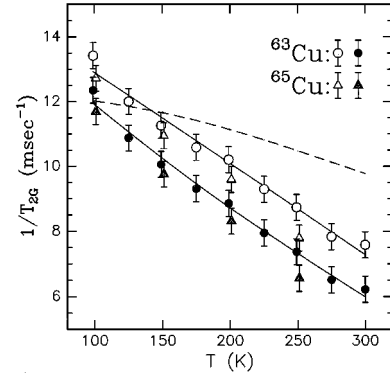


FIG. 2. Uncorrected (open symbols, T_{2G}^{-1}) and corrected (filled symbols, T_{2GS}^{-1}) echo decay rate parameters for both isotopes of copper in LSCO are plotted as a function of temperature. The solid lines are spline fits to the ⁶³Cu data. The dashed line is a calculated curve based on recent neutron data (Ref. 3) and assumed model temperature and frequency dependences as described in the text.

polated linearly for temperatures in between. The effect of the background term may be gauged by comparing the fitted values for T_{2G} with estimates obtained by simply correcting the raw data (Fig. 1) with the T_{1Ec} factor [Eq. (1)] and taking the initial slope of the resulting data plot as T_{2G}^{-2} . The “correction” to T_{2G} estimated in this way is $\sim 5\%$ at $T=100$ K and declines in importance at higher temperatures. It is negligible for $T \geq 200$ K.

In performing a data fit based on Eq. (1), then, the only fitting parameters are A and T_{2G} . The resulting fits are very good (Fig. 1, solid curves), where the Gaussian decay forms so obtained are shown as dashed lines. The greatest systematic uncertainty in these results comes from the estimates of T_{1Ec} , particularly at higher temperatures. T_{2G} data from fits such as these are plotted for both isotopes in Fig. 2 as open symbols. As found earlier,⁷ experimental decay rates for the two copper isotopes are nearly the same. This observation was explained by detailed calculations presented in Ref. 7, which we now summarize briefly.

The relevant indirect coupling Hamiltonian terms for the copper spins were shown to have the form

$$\mathcal{H} = \sum_{i>j} \alpha_{ij} I_{zi}^A I_{zj}^A + \sum_{i>j} \delta_{ij} \vec{I}_i^A \cdot \vec{I}_j^A + \sum_{j,k} \beta_{jk} I_{zj}^A I_{zk}^B + \sum_{k,l} \gamma_{kl} \vec{I}_k^B \cdot \vec{I}_l^B, \quad (2)$$

where the A (B) spins are the Cu spins which are (are not) being observed. The B -spins include all spins of the “other” isotopes,¹⁴ plus members of the observed species which are found instantaneously in the $m_i = \langle I_{zi}^A \rangle = \pm \frac{3}{2}$ state. The A -spin second moment is determined by the α_{ij} and β_{ij} terms, while the exchange-like δ_{ij} (γ_{kl}) terms cause spin-spin flip-flops among the $m = \pm \frac{1}{2}$ A (B) spins. The combined effects of these flip-flop transitions and of T_1 transitions is to modify and in most cases to shorten the spin-echo decay process. Using experimental T_1 values we have calculated decay rates T_{2G}^{-1} as a function of the flip-flop transition rate $\Delta W_{\pm 1/2}$ between the $\pm \frac{1}{2}$ states. The latter results are shown in the inset to Fig. 3 for a typical case, where we have plotted a dimensionless correction factor ${}^{63}T_{2GS}/T_{2G}$ as a function

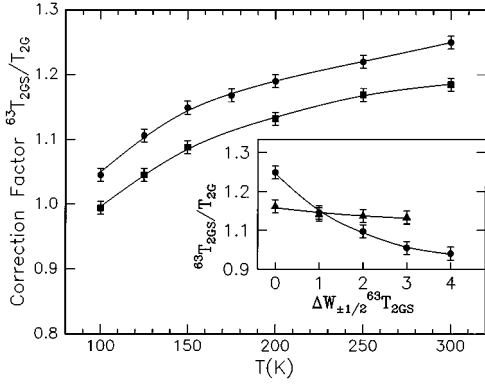


FIG. 3. Correction factors ${}^{63}T_{2GS}/T_{2G}$ for ${}^{63}\text{Cu}$ in both LSCO (dots) and YBCO (squares) are plotted as a function of temperature. These data are obtained from Gaussian fits to decay curves calculated as described in Ref. 7. T_1 values and time intervals over which fits are made correspond to actual experimental conditions as discussed in the text. The inset shows variations of the calculated correction factor with assumed flip-flop transition rate $\Delta W_{\pm 1/2}$ for the two isotopes at $T \sim 150$ K. The crossing at $\Delta W_{\pm 1/2} \approx {}^{63}T_{2GS}^{-1}$ gives the observed correspondence ${}^{63}T_{2G} \approx {}^{65}T_{2G}$; this condition varies only slightly over the range of temperatures studied.

of $\Delta W_{\pm 1/2}$, which is given in units of ${}^{63}T_{2GS}^{-1}$. For $\Delta W_{\pm 1/2} \approx {}^{63}T_{2GS}^{-1}$ the decay rates for the two isotopes are observed to cross, giving the observed result (Fig. 2) ${}^{63}T_{2G} \approx {}^{65}T_{2G}$. This value for $\Delta W_{\pm 1/2}$, which we adopt here throughout, is in agreement with rough estimates.¹⁵ The correction factor ${}^{63}T_{2GS}/T_{2G}$ is then shown in Fig. 3 as a function of temperature for the case of LSCO.¹⁶ We also show results for YBCO for the experimental conditions described in Ref. 12, where we have assumed the anisotropy of the indirect coupling is the same for both systems. The corrections are seen to be slightly larger for LSCO, but to vary with temperature over a range of $\sim 20\%$ in both cases.

On applying the correction factor for LSCO (Fig. 3) to the raw T_{2G} data in Fig. 2, we obtain estimates of the static decay rate T_{2GS}^{-1} (solid points), which is given directly by the calculated indirect coupling.¹¹ The dipolar second moment contribution is two orders of magnitude smaller than $\langle \Delta \omega^2 \rangle_{\text{ind}}$ for the copper case and is thus neglected. Values of T_{2GS} are seen to vary by a factor ~ 2 over the temperature range studied. It is interesting to compare this behavior with that of T_{2GS} for YBCO. Using the data reported in Ref. 12 and the calculated corrections in Fig. 3, T_{2GS} is found in this case to vary in a similar fashion, but by slightly less than a factor of 2. Interestingly, a very similar variation is also found for T_1T (${}^{63}\text{Cu}$) for these two systems, i.e., nearly a factor of 2 over this temperature interval for LSCO (Refs. 4,5) and slightly less than that for YBCO.¹² We find it somewhat surprising, then, that Sokol and Pines¹³ have categorized these compounds as having a different dynamical exponent z .

We reexamine this point in some detail here, using the criteria¹³ that T_1T/T_{2GS} and T_1T/T_{2GS}^2 are independent of temperature for $z=1$ and 2, respectively. Using T_{2GS} data from Fig. 2 and T_1T from Ref. 5 for LSCO and corresponding data from Ref. 12 for YBCO, we plot both T_1T/T_{2GS} and T_1T/T_{2GS}^2 vs T in Fig. 4. Corrected and uncorrected T_{2G} data

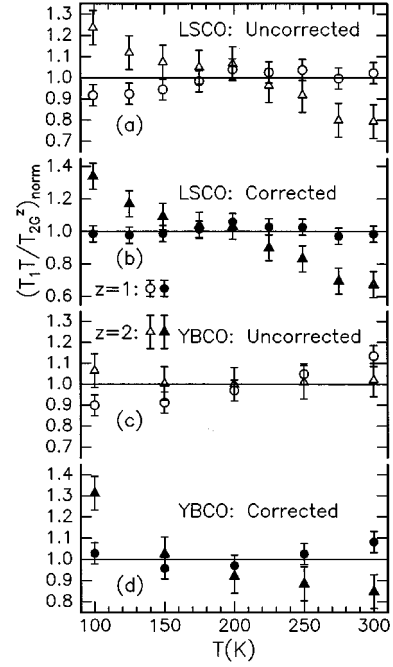


FIG. 4. Plots of T_1T/T_{2G} (dots) and T_1T/T_{2G}^2 (triangles) as a function of temperature are shown, using uncorrected (open symbols) and corrected (filled symbols) for both LSCO and YBCO as indicated. The data for YBCO are taken from Ref. 12. For LSCO the T_1 data are from Ref. 4 and the $T_{2G(S)}$ data are from Fig. 2.

for both LSCO and YBCO are shown as indicated in the figure. For LSCO the corrected data make a clear case for $z=1$, where the uncorrected data are similar, but somewhat murkier. For YBCO, however, the uncorrected data appear to favor the $z=2$ (overdamped) case.¹³ After correcting the T_{2G} data by the amounts shown in Fig. 3, however, the $z=1$ case appears to be flatter with temperature [Fig. 4(d)]. These results, as well as the general similarity in relaxation behavior of LSCO and YBCO, are good evidence that they should both be placed in the $z=1$ (quantum disordered) category.¹⁷

It is interesting to compare our results for the temperature dependence of T_{2GS} (Fig. 2) with estimates based on recent neutron-scattering data for LSCO.³ To do this we use the KK relation $\chi'(\vec{q}) = \int_0^\infty d\omega \chi''(\vec{q}, \omega)/\omega$ to estimate $\chi'(\vec{q})$, which is then Fourier transformed and combined with hyperfine constant data to generate the indirect nuclear spin-spin couplings^{7,8} and estimates of $T_{2GS}(T)$. In practice this procedure is somewhat speculative, because data for $\chi''(\vec{q}, \omega)$ are only available over a limited range of energies. We proceed, then, by adopting a hypothetical temperature variation for the profile of $\chi''(\vec{q}, \omega)$ vs ω which is suggested by the low-energy data. The calculation is to some extent a test of this hypothetical form.

With the foregoing picture in mind, we proceed to implement the KK integral given above as follows, using data from Ref. 3. We adopt the functional form $\chi''(\vec{q}, \omega) = \chi_0''(\omega, T) \kappa^4 / [\kappa^2 + R(\vec{q})]^2$, where $\chi_0''(\omega, T)$ is the peak amplitude, $\kappa(\omega, T)$ is the inverse correlation length, and the \vec{q} dependence is controlled by $R(\vec{q}) = \{[(q_x - q_y)^2 - \delta^2 \pi^2]^2 + [(q_x + q_y)^2 - \delta^2 \pi^2]^2\} / (8a_0^2 \pi^2 \delta^2)$. Here a_0 is the

lattice constant and $\delta=0.245$ is the incommensurability parameter. From Ref. 3 we also have $\kappa^2 a_0^2 = 0.0167 + [(\hbar\omega)^2 + (k_B T)^2]/E_0^2$, determined at energies up to 15 meV, where $E_0 = 47$ meV. In Ref. 7 we modeled $\chi''_0(\omega, T)$ vs ω at $T=100$ K as rising linearly to a maximum at ω_{peak} , then remaining flat to a cutoff energy ω_{co} . Using the observed behavior at $T=35$ K, we set $\hbar\omega_{\text{peak}} \approx 2.3k_B T = 20$ meV. The value of ω_{co} was adjusted in the KK integral to yield the measured value of T_{2GS} for ⁶³Cu, giving $\hbar\omega_{\text{co}} \approx 46$ meV at $T=100$ K.

Here, we seek to extend the KK estimate of $\chi'(\vec{q})$ to higher temperatures, in order to obtain a calculated temperature variation $T_{2G}(T)$ which is consistent with available neutron data for $\chi''(\vec{q}, \omega)$. Our main assumptions are: (1) The variation $\chi''(\vec{q}, \omega) \propto T^{-2}$ from the analysis in Ref. 3; (2) we take $\omega_{\text{peak}}(T) \propto T$ as suggested by the low-temperature data; and (3) the cutoff $\omega_{\text{co}}(T)$ is determined by the global sum rule on $\chi''(\vec{q}, \omega)$ discussed by Millis and co-workers,¹⁰

$$SR = \sum_q \int_0^\infty d\omega \chi''(\vec{q}, \omega) (1 - e^{-\hbar\omega/kT}) = \mu_B^2 \langle s_\alpha^2 \rangle, \quad (3)$$

where Σ_q is a normalized sum and $\langle s_\alpha^2 \rangle$ is evaluated over relevant states for a single fermion. One expects $\langle s_\alpha^2 \rangle = 0.25$ for a localized moment, and slightly smaller values¹⁰ for itinerant fermions. Since Eq. (3) was not employed in earlier work, we describe briefly its implications for modeling energy profiles for $\chi''(\vec{q}, \omega)$. For the parameters (ω_{peak} , ω_{co}) employed to interpret T_{2G} in Ref. 7 (see above), one finds $SR = 0.36$. This is somewhat too large, but well within the error limits of experimental parameters. For

example, if we reduce ω_{co} to 37 meV for $T=100$ K, then $SR \sim 0.25$. The consequent change in T_{2G} can be compensated by scaling the hyperfine parameters by $\sim 10\%$, which is within experimental uncertainty. Since the sum rule must always be satisfied, we use the condition $SR = 0.36$ to determine $\omega_{\text{co}}(T)$ at temperatures from 100 K up to room temperature.¹⁸ The resulting parameters are then used to calculate $\chi'(\vec{q})$ and T_{2G} using the same hyperfine parameters as in Ref. 7. The results are plotted in Fig. 2 as a dashed line.

Correspondence with the experimental data is only fair, showing, however, a modest downtrend over most of the temperature range. Evidently, there are significant deviations from the simple energy and temperature scaling assumptions used in this calculation. Interestingly, however, the calculated curve for $T_{2GS}(T)$ does not show the serious discrepancy found between $\chi''(\vec{q}, \omega)$ and the T_1 data,³ and leaves open the possibility that more complete neutron data will lead to a better account of the T_{2GS} results. In such a case, the discrepancy with high-temperature T_1 data will begin to look more serious, with its startling implication that for the metallic phase, T_1 at high temperatures is dominated by something other than the traditional paramagnetic spin fluctuation mechanism.

In summary, we find that there are significant corrections to the measured spin-echo decay times from both T_1 and spin-spin coupling dynamics for both YBCO and LSCO. Appropriate corrections have been calculated, and the corrected estimates of indirect spin-spin coupling for both of these systems suggest that they are in the quantum disordered ($z=1$) category. $T_{2GS}(T)$ for LSCO is also found to be consistent with recent neutron data extending up to room temperature.

¹S-W. Cheong *et al.*, Phys. Rev. Lett. **67**, 1791 (1991); T. E. Mason, G. Aeppli, and H. Mook, *ibid.* **68**, 1414 (1992).

²M. Matsuda *et al.*, Phys. Rev. B **49**, 6958 (1993).

³G. Aeppli, T. E. Mason, S. M. Hayden, and H. A. Mook (unpublished).

⁴T. Imai *et al.*, J. Phys. Soc. Jpn. **59**, 3846 (1990).

⁵R. E. Walstedt, B. S. Shastry, and S-W. Cheong, Phys. Rev. Lett. **72**, 3610 (1994).

⁶L. Reven *et al.*, Phys. Rev. B **43**, 10466 (1991).

⁷R. E. Walstedt and S-W. Cheong, Phys. Rev. B **51**, 3163 (1995).

⁸C. H. Pennington and C. P. Slichter, Phys. Rev. Lett. **66**, 381 (1991).

⁹B. S. Shastry, Phys. Rev. Lett. **63**, 1288 (1989).

¹⁰A. J. Millis, H. Monien, and D. Pines, Phys. Rev. B **42**, 167 (1990); A. J. Millis and H. Monien, *ibid.* **45**, 3059 (1992).

¹¹Static echo decay refers to conditions where all spin-lattice or spin-spin fluctuation processes are negligible on the time scale of T_{2G} .

¹²T. Imai, C. P. Slichter, A. P. Paulikas, and B. Veal, Phys. Rev. B **47**, 9158 (1993).

¹³A. Sokol and D. Pines, Phys. Rev. Lett. **71**, 2813 (1993).

¹⁴Copper has two isotopes, ⁶³Cu and ⁶⁵Cu, both with $I = \frac{3}{2}$, and with abundances of 0.691 and 0.309, respectively.

¹⁵A simple calculation shows that the rms matrix element for a spin-flip transition of a pair of spins, driven by the δ_{ij} term in Eq.

(2), is $[(f/8)\Sigma_{j(\neq i)}\delta_{ij}^2]^{1/2}$, where f is the isotopic abundance and Σ_j covers the entire lattice. We use this as an estimate of the corresponding rate. The expression in square brackets is recognizable as that for the second moment $\langle \Delta\omega^2 \rangle_A$ (Ref. 7) with δ_{ij} substituted for α_{ij} [see Eq. (2)]. Using $T_{2GS}^2 = 2/\langle \Delta\omega^2 \rangle_A$, we find $\Delta W_{\pm 1/2} T_{2GS} \approx 2\sqrt{2}[\Sigma_{j(\neq i)}\delta_{ij}^2/\Sigma_{j(\neq i)}\alpha_{ij}^2]^{1/2}$. Numerical results (Ref. 7) give $\Sigma_{j(\neq i)}\delta_{ij}^2 \approx \Sigma_{j(\neq i)}\alpha_{ij}^2/4$, whereupon we have $\Delta W_{\pm 1/2} T_{2GS} \approx \sqrt{2}$. The slightly smaller value found in practice may result from the presence of the α_{ij} terms, which have been ignored in this estimate.

¹⁶The correction factors given in Fig. 3 are defined as the slope of $\ln[\mathcal{E}(\tau)]$ vs τ^2 divided by the same slope for the case of static spins observed with a $\pi/2$ - π pulse sequence, where $\mathcal{E}(\tau)$ is the echo amplitude. Since the T_1 effect on $\mathcal{E}(\tau)$ produces a slight downward curvature on the decay curve, the perceived slope, and thus correction factor, depends to the extent of a few percent on the τ interval over which it is defined. The corrections given in Fig. 3 were obtained by fitting straight lines to calculated decay curves over ranges of τ corresponding to the experimental data for LSCO (Fig.1) and YBCO (Ref. 12).

¹⁷See, however, other criteria for the assignment of z values in (Ref. 13).

¹⁸The temperature dependence resulting from this condition is not strongly dependent on the value chosen for the sum rule.